

# Analysis of failure mechanisms in velocity-matched distributed photodetectors

A. Nespola  
T. Chau  
M.C. Wu  
G. Ghione

**Abstract:** The thermal-runaway process in long-wavelength velocity-matched distributed photodetectors (VMDP) with metal-semiconductor-metal photodiodes has been investigated. A three-dimensional numerical electrothermal model has been developed which takes into account the nonlinear thermal properties of the substrate and the nonuniform temperature rise due to self heating. The model shows that, owing to its distributed nature, the photodetector is able to operate at high optical-power level before catastrophic failure occurs. When this happens, a highly localised hot spot appears within the device and the  $I$ - $V$  characteristic exhibits a typical 'current crush point', where the current rapidly increases with increasing bias voltage. Examples are discussed to highlight the thermal behaviour of the distributed detector and to compare the model with experimental data.

## 1 Introduction

High-power high-speed photodetectors are attractive devices for applications in optical-heterodyne detection in the microwave- and millimetre-wave range. Moreover, they are key components in microwave fibre-optic links whose performance parameters (such as the link gain, signal-to-noise ratio and spurious free dynamic range) benefit from receiving the maximum available optical power [1]. Significant progress has been made in this kind of photodetector using both surface-illuminated [2, 3] and waveguide approaches [4]; however, the small absorption volume, required for high-speed operation, causes the density of photogenerated carriers to be high even at low input optical power. The ensuing electric-field screening effects lead to low saturation power, nonlinear behaviour and harmonic distortion.

Enlarging the effective absorption volume is the most direct way of increasing the saturation power. To achieve high-power capabilities with high bandwidth

and efficiency, travelling-wave photodetectors, first suggested in [5], have been used [6, 7]. Although their increased absorption volume enables good saturation levels to be obtained, very low bandwidth has been reported (4.8GHz) because of the difficulty of matching the velocities of the copropagating optical and electrical waves [7].

To overcome this problem and to take advantage of the travelling-wave concept, a GaAs/AlGaAs velocity-matched distributed photodetector (VMDP) is proposed which operates at 860nm [8]; a high saturation photocurrent of 56mA and a bandwidth of 49GHz have been achieved. However, InP-based long-wavelength photodetectors, operating at 1.3 and 1.55 $\mu$ m, are required in long-haul photonic systems. Recently, the first experimental results on InGaAs/InAlAs/InP VMDP were reported [9]. Its structure and physical behaviour are discussed in detail below.

Since VDMPs are high-power detectors, device breakdown induced by thermal runaway is a potentially serious problem, and a quantitative failure model is needed to improve the device performance and reliability. In this paper, the thermal runaway process that leads to catastrophic damage in InP-based photodetector is investigated through a self-consistent steady-state electrothermal model. To obtain high-resolution surface-temperature maps at a moderate computational cost, Green's-function approaches, coupled with efficient numerical implementations, have been exploited. Thermal runaway is assumed as an indicator for potential device failure, since the actual failure mechanism (metal diffusion into the semiconductor, which ultimately leads to photodiode short-circuiting), is activated by a temperature increase.

## 2 Design and fabrication

The schematic structure of the VMDP is illustrated in Fig. 1. High-speed metal-semiconductor-metal (MSM) photodiodes, chosen because of their easy integration with microwave transmission lines, are periodically distributed on top of a passive optical waveguide. The output photocurrents are collected by a 50 $\Omega$  coplanar-strip (CPS) microwave transmission line that is velocity matched to the optical waveguide.

Each active MSM photodiode consists of an InGaAs absorption layer, InGaAs/InAlAs graded superlattice layers, InAlAs Schottky-barrier enhancement layer, and Ti/Au fingers with thickness of 200 $\text{\AA}$ /2000 $\text{\AA}$ . The mesa is defined by wet etching down to the InAlAs upper cladding II. Fig. 2 shows the cross-section of VMDP after mesa etching and an enlarged image of graded superlattice which consists of 11 pairs of alter-

© IEE, 1999

IEE Proceedings online no. 19990457

DOI: 10.1049/ip-opt:19990457

Paper first received 9th June and in revised form 28th October 1998

A. Nespola and G. Ghione are with Politecnico di Torino, Dipartimento di Elettronica, Corso Duca degli Abruzzi 24, I-100129 Torino, Italy

T. Chau and M.C. Wu are with UCLA, Electrical Engineering Department, 66-147-D Engineering IV, Los Angeles, CA 90095-1594, USA

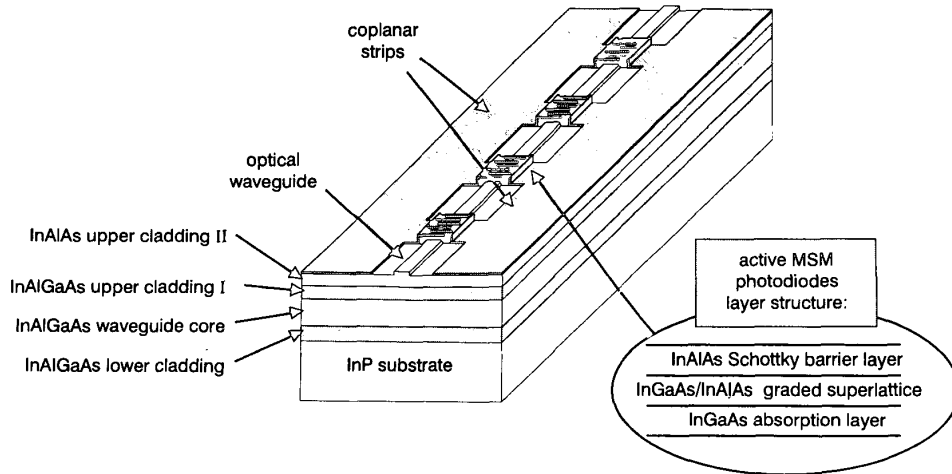


Fig. 1 Schematic structure of long-wavelength velocity-matched distributed photodetectors (VMDP)

nate layers of  $\text{In}_{0.53}\text{Ga}_{0.47}\text{As}$  and  $\text{In}_{0.52}\text{Al}_{0.48}\text{As}$  with thickness gradually varied in opposite directions from  $55\text{ \AA}$  to  $5\text{ \AA}$  with a fixed period of  $60\text{ \AA}$ . The absorbing region is designed to be on the top surface and evanescently coupled to a  $3\text{ }\mu\text{m}$ -wide optical-ridge waveguide which is defined by further etching down  $0.1\text{ }\mu\text{m}$  of the InAlAs upper-cladding II layer. The material composition and thickness of each layer is designed in such a way that only the optical fundamental mode exists in both the passive waveguide and active photodiode region. After mesa and waveguide etching, the interdigitated fingers and the coplanar-strip microwave transmission lines are patterned using a standard liftoff technique.

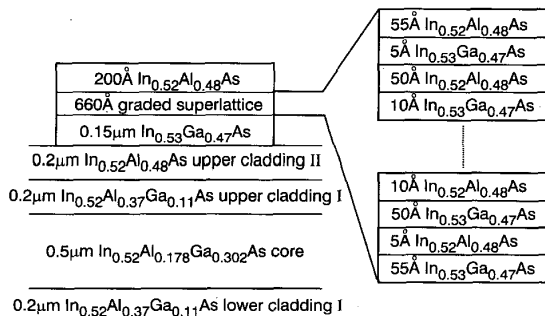


Fig. 2 Schematic cross-section of VMDP after mesa etching

The VMDP design allows the passive waveguide, the active photodiodes, and the microwave coplanar strips to be optimised independently. The optical waveguide is designed for low coupling loss and single-mode operation. All photodiodes are kept below saturation by coupling a small portion of the optical power from the waveguide. The microwave transmission line is optimised for impedance and velocity matching without sacrificing the photodiode performance. Finally, in addition to their photoactive action, the periodically arranged MSM structure is also used as shunt capacitive load of the CPS line, required to slow the speed of the electrical wave with respect to the optical one, thus achieving the velocity match. Although the quantum efficiency of each MSM is kept low to allow for high saturation power, the photocurrents are summed in

phase and the total quantum efficiency of the VMDP increases with the increasing number of photodiodes, thanks to the velocity match and series connection.

The first experimental  $1.2\text{mm}$ -long device, consisting of 12 MSM photodiodes, exhibited a  $3\text{dB}$  bandwidth of  $18\text{GHz}$  and an overall quantum efficiency of  $34\%$  [9]. Optical lithography is employed to pattern the MSM photodiodes, and the resulting finger width and spacing are both  $1\text{ }\mu\text{m}$ . Thus, by scaling down the MSM to  $0.1\text{ }\mu\text{m}$  through EB lithography, a frequency response in excess of  $100\text{GHz}$  is expected.

### 3 Electrothermal-modelling approach

The operation of high-power VMDP is characterised by a significant amount of device self heating. In addition to affecting the VMDP reliability and lifetime, a catastrophic temperature increase caused by thermal runaway can occur. Strong device heating is expected to activate technology-dependent degradation mechanisms (such as metal diffusion) which ultimately lead to device failure. Thus, the thermal-runaway condition can be expected to be a significant indicator of device failure, even if the detailed failure mechanism is not explicitly included in the model. A self-consistent model for the device temperature distribution and a quantitative understanding of the operating conditions leading to thermal runaway are therefore useful for improving device design.

A simple thermal-runaway mechanism in VMDPs can be associated with the temperature increase of the reverse dark current. This additional current will in turn generate heat, thus leading to positive feedback. At some point, commonly defined as the 'current crush point', the process becomes unstable, resulting in uncontrolled current and temperature rise until catastrophic failure occurs [10]. To model the process, the temperature dependence of the dark current and the temperature distribution associated with Joule heating must be investigated.

Since the MSM photodiode consists basically of two Schottky contacts connected back to back, it is only possible to measure the reverse  $I$ - $V$  characteristics, even if the bias voltage  $V$  is positive. The dark-current-voltage relationship can be analysed by using a thermionic-emission model and by superimposition of the single MSM solutions [11]:

$$I_j^{dark} = SA^* \exp\left(\frac{-q\phi}{KT_j}\right) \exp\left(\frac{-qV}{\gamma KT_j}\right) \times \left\{ \exp\left(\frac{qV}{KT_j}\right) - 1 \right\} \quad (1)$$

$$I^{dark} = \sum_{j=1}^N I_j^{dark} \quad (2)$$

where  $N$  is the number of MSM detectors in the VMDP device and  $T_j$  is the average temperature on the  $j$ th MSM. Since all MSM detectors have the same size and structure, the contact area  $S$ , the modified Richardson's constant  $ASUP^*$  and the Schottky-barrier height  $\phi$  have been handled as constant throughout the VMDP. The effect of the image-force lowering has been taken into account through the ideality factor  $\gamma$ . The dark current measured under DC bias by connecting the device to a heat sink at temperature  $T$  does not lead to significant Joule heating, i.e.  $T_j = T$  for all MSM detectors. On the basis of this assumption, the dark currents of the VMDP have been experimentally characterised for various bias voltages and temperatures, and then fitted to the model in eqns. 1 and 2, as shown in Fig. 3 for a 1.2mm-long VMDP consisting of eight  $16 \times 48 \mu\text{m}^2$  MSM photodiodes. Values around 0.6eV and  $7.74 \text{A}/\text{cm}^2\text{K}^2$  have been found for the barrier height and Richardson's constant, respectively; these values are close to the values suggested for the same epitaxial structure by Lee and Sheng Li [12]. The ideality factor  $\gamma$  is around 1.007.

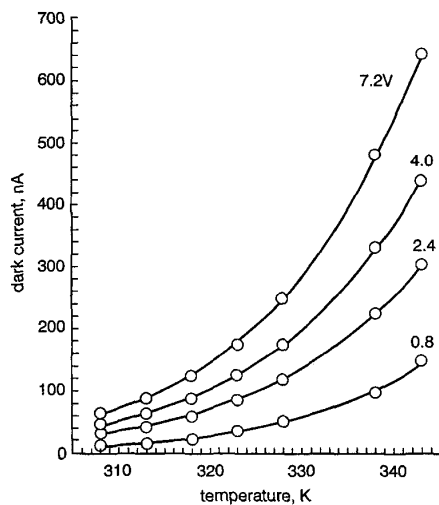


**Fig. 3** Dark current against temperature for a 1.2mm-long VMDP device with eight  $16 \times 48 \mu\text{m}^2$  MSM photodiodes  
— simulation  
○ experimental data

The effective refractive index (ERI) and the multi-layer stack theory [13] are exploited to compute the optical-field profile. The transverse structure is multimodal along the lateral direction ( $y$  axis) only; Figs. 4 and 5 provide examples of the optical-field profiles for the fundamental mode in the active region and the passive waveguide, respectively. The optical wave is mainly confined in the passive core region, and is coupled evanescently to the top InGaAs absorbing region in the active section. The confinement factor is very low ( $\Gamma = 2.3$ ) in agreement with the purpose of high-power operation. Since the optical transitions between the passive

waveguide and the active photodiode sections are relatively smooth, the theoretical coupling efficiency  $K_1$  for the designed VMDP is found to be 98%. Further, the structure is designed to guarantee a high coupling efficiency ( $K_0 = 68.4$ ) between the waveguide mode and the Gaussian field emitted by a single-mode fibre. Assuming  $P_o$  to be the optical input power coupled into the VMDP photodetector, the photocurrent developed by the  $j$ th MSM detector can be expressed as

$$I_j^{ph} = P_o K_0 \{K_1(1-\eta)K_1\}^{j-1} K_1 \eta \quad (3)$$

where  $\eta$  is the quantum efficiency of the single MSM photodiode while the propagation in the passive optical waveguide is assumed to be lossless.

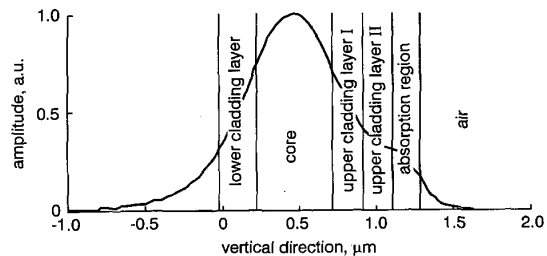


**Fig. 4** Optical-field profile in the active photodiode region of the VMDP

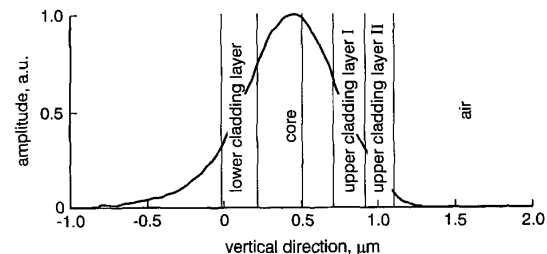


**Fig. 5** Optical-field profile in the passive waveguide region of the VMDP

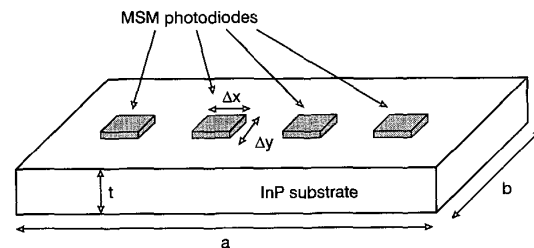


**Fig. 6** Schematic diagram of a VMDP with four flat MSMs

To find the temperature distribution of the device, a numerical, three-dimensional thermal model has been developed. Fig. 6 shows a schematic diagram of a VMDP device where each MSM photodiode is modelled as a rectangular source on top of the InP substrate;  $a$ ,  $b$  and  $t$  are, respectively, the  $x$ ,  $y$  and  $z$  dimensions of the substrate. No heat flow through the sides, end facets or top surface of the substrate is considered. The heat generated by the MSM photodiodes is removed by a highly conductive sink, which is kept at room temperature  $T_0$ . With these boundary conditions, the thermal-resistance matrix of the substrate can be computed efficiently thanks to spectral-domain Green's-function techniques coupled with FFT methods, including the effect of surface metallisation [14, 15] and the nonlinear thermal-substrate properties [16].

Nevertheless, the influence of heat conduction through the thin surface metal on the surface temperature distribution has been found to be negligible in the devices under investigation. A simple iterative numerical scheme is used to obtain a self-consistent solution of the temperature distributions and  $I-V$  characteristics: given the external bias and optical input power, an initial guess is provided for the average temperature of each MSM detector and the current is evaluated as sum of the dark and photocurrent. From the distribution of the dissipated power, a new guess is computed for the average temperature increase on each MSM detector. The iterative process is repeated until, for each source, the temperature change between consecutive iterations is smaller than 0.1 K. After convergence, an increased value of bias voltage is proposed as the starting point for a new iteration.

#### 4 Discussion and results

Fig. 7 shows the calculated  $I-V$  characteristics for two different devices, denoted as VMDP1 and VMDP2. The first is a  $400\mu\text{m}$ -long device with four  $11 \times 48\mu\text{m}^2$  MSM photodiodes, while VMDP2 is a  $600\mu\text{m}$ -long device with four  $16 \times 48\mu\text{m}^2$  MSMs. The theoretical quantum efficiency  $\eta$  of each individual MSM photodiode is 7.6% in device VMDP1 and 11.2% in VMDP2. For an optical input power of 500mW, VMDP2 has a breakdown voltage of around 16V and the corresponding damaging electrical power level is around 2.3W. As the size of MSM photodiodes is reduced, the thermal power generated decreases and the runaway process occurs at a higher voltage. However, the advantage gained is comparatively small, and does not compensate for the reduction in output power caused by the lower output current (see Fig. 7).

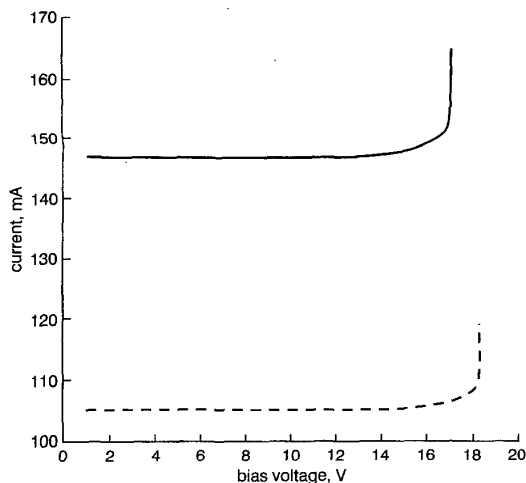


**Fig. 7** Theoretical  $I-V$  characteristics of VMDP1 consisting of four  $11 \times 48\mu\text{m}^2$  MSMs, and VMDP2 consisting of four  $16 \times 48\mu\text{m}^2$  MSMs. Optical input power = 500mW. Both photocurrent and thermally-dependent dark current have been considered.

The temperature distributions at the top surface of VMDP2, under 500mW optical power, are shown in Figs. 8 and 9 for bias voltages of 12V and 17V, respectively. At the first operating point (12V) the temperature variations are small across the four detectors. At 17V thermal runaway has taken place and the tempera-

ture distribution shows a dramatic difference between the first MSM (where a highly localised hot spot is formed) and the others. This is, of course, consistent with the fact that in the present VMDP design the optical power absorbed by the first MSM detector is significantly larger than the power absorbed by the other detectors. Therefore, if the size of photodiodes is fixed but their number is increased, the current crush point for the first MSM and for the whole VMDP remain the same, but the total photocurrent increases.

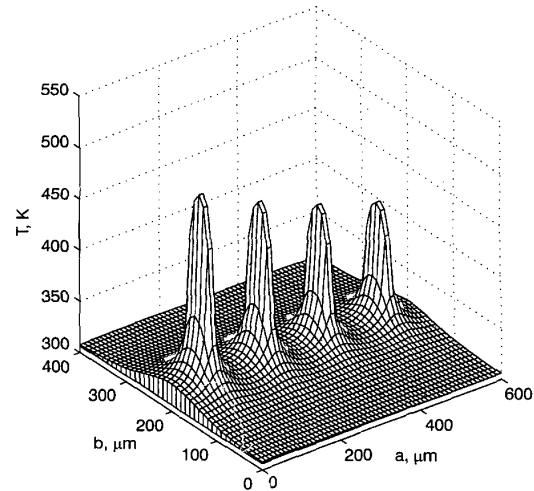


**Fig. 8** Temperature distribution on surface of substrate for  $600\mu\text{m}$ -long (axis  $a$ ), and  $400\mu\text{m}$  wide (axis  $b$ ) device with four MSM photodiodes ( $16 \times 48\mu\text{m}^2$ ) for optical power of 500mW and voltage of 12V

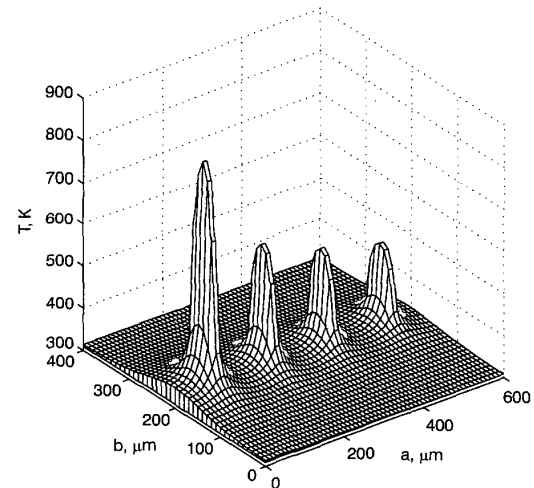


**Fig. 9** Temperature difference on surface of substrate for  $600\mu\text{m}$ -long (axis  $a$ ), and  $400\mu\text{m}$  wide (axis  $b$ ) device with four MSM photodiodes ( $16 \times 48\mu\text{m}^2$ ) for optical power of 500mW and voltage of 17V

The advantage achieved by the distributed structure compared with a concentrated one in terms of thermal behaviour clearly appears on comparing the theoretical  $I-V$  characteristics of VMDP2 and of a lumped MSM photodetector with the same active area (see Fig. 10); the input optical power is 500mW for both structures. Although the same DC quantum efficiency is obtained in both structures, the breakdown voltage of the VDMP shows a dramatic improvement.

Despite the excellent performances of VMDPs, the application of such devices to real-world systems can be compromised by poor reliability. In fact, even if the

VMDP bias and optical input power are kept well below the thermal-runaway condition, the device peak temperature could still reach 450K (see Fig. 8); this is of great concern when assessing VMDP reliability and lifetime, since degradation mechanisms are well known to be exponentially accelerated by an increase of the operating temperature. The fact that high-temperature tests in the range 370–470K are generally used to reduce test-time aging rates by several orders of magnitude suggests that a temperature of 450K is certainly of concern. Furthermore, degradation of metal contacts associated with their reaction with semiconductor surface layers is expected to be a typical failure mechanism, as it is in temperature-accelerated testing [17]. It is also expected that reaction between metal and III–V compound semiconductors will ultimately form alloys of metal–III elements and of metal and III–V elements. Such processes, involving interdiffusion, result in the generation of defects and an increase in thermal and electrical resistance.

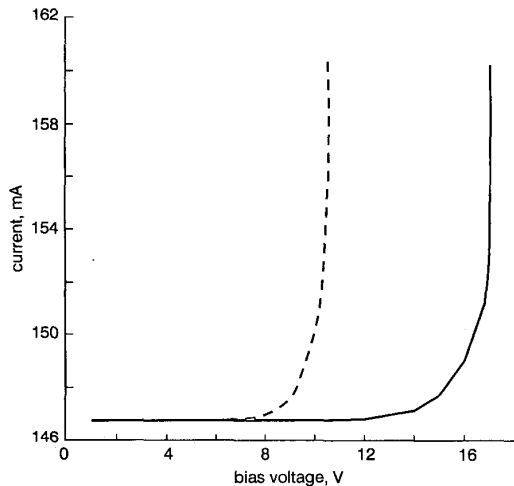


**Fig. 10** Comparison between theoretical  $I$ - $V$  characteristic of VMDP2 and of single MSM with same total active area and total quantum efficiency (at low frequency)  
 --- single MSM  
 — VMDP2  
 Optical input power = 500mW  
 Current includes photocurrent and thermally dependent dark current

In the present device, the failure mechanism appears to be dominated by the diffusion of metals from electrode to semiconductor. A few VMDP devices were stressed intentionally (gradually increasing optical power and bias) and an electrical-power level was measured at breakdown of 50mW. Clear signs of gold diffusion into the semiconductor material were found. For all devices tested to failure, visual inspection showed that the first photodiode at the input end was most severely damaged, and there was no observable damage for subsequent photodiodes. This confirms what is predicted by the theoretical model. The scanning-electron micrograph (SEM) of a failed device is shown in Fig. 11, in which the degradation of the MSM fingers is clearly visible. The technological limitation due to gold diffusion could be overcome using Pt/Ti/Pt/Au as the Schottky metal instead of Ti/Au; in fact Pt has been proven to be better as a diffusion barrier for gold, besides having a higher Schottky barrier. Apart from technology improvements, the thermal and reliability properties of the device can also be improved by decreasing the size of the first detector (to reduce its

thermal-power dissipation), and by gradually increasing the size of the other MSM detectors, to achieve comparable or better quantum efficiency. A new design incorporating such improvements is in progress.

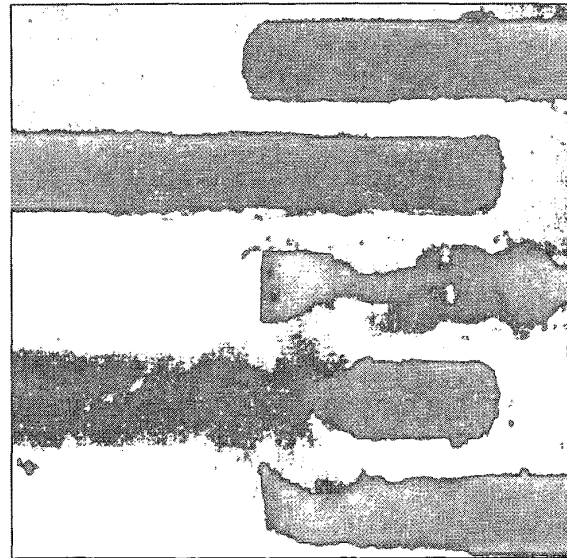


**Fig. 11** SEM picture of first photodiode of failed VMDP

## 5 Conclusions

A thermal-runaway analysis for velocity-matched distributed photodetectors (VMDP) has been developed through the help of a coupled electrothermal-device model. The presence of temperature-activated degradation mechanisms (above all in the MSM structures) suggests that thermal runaway can be assumed as a fair indicator of potential catastrophic failure. The electrical power level at which thermal-runaway occurs has been shown to be improved dramatically by the use of a distributed structure; moreover, higher power levels can also be achieved by increasing the number of MSM photodetectors, since failure has been shown to occur on the first (front-end) stage, where the maximum input optical power is detected. Also below thermal-runaway, VMDPs have been found to have high operating temperatures, which are expected to be of concern in assessing device reliability. Diffusion of gold into semiconductor has been experimentally shown to be a major cause of catastrophic failure in actual devices.

## 6 Acknowledgments

This project is supported by TRW, ONR, MURI on RF Photonics, ARO, JSEP, and UC MICRO.

## 7 References

- 1 COX, C.H.: 'Gain and noise figure in analogue fiber-optic links', *IEE Proc. J. Optoelectron.*, 1992, **139**, (4), pp. 238–242
- 2 WEY, Y.G., GIBONEY, K., BOWERS, J., RODWELL, M., SILVESTRE, P., THIAGARAJAN, P., and ROBINSON, G.: '110 GHz GaInAs/InP double heterostructure  $p$ - $i$ - $n$  photodetectors', *J. Lightwave Technol.*, 1995, **13**, (7), pp. 1490–1499
- 3 CHOU, S.Y., and LIU, M.Y.: 'Nanoscale tera-hertz metal-semiconductor-metal photodetectors', *IEEE J. Quantum Electron.*, 1992, **28**, (10), pp. 2358–2368
- 4 KATO, K., KOZEN, A., MURAMOTO, Y., ITAYA, Y., NAGATSUMA, T., and YAITA, M.: '110 GHz, 50% efficiency mushroom-mesa waveguide  $p$ - $i$ - $n$  photodiode for a 1.55  $\mu$ m wavelength', *IEEE Photonics Technol. Lett.*, 1994, **6**, (6), pp. 719–721

- 5 TAYLOR, H.F., EKNOYAN, O., PARK, C.S., CHOI, K.N., and CHANG, K.: 'Traveling wave photodetectors'. Proceedings of SPIE conference *Optoelectronic signal processing for phased-array antennas II*, 1990, Vol. 1217, pp. 59-63
- 6 GIBONEY, K.S., RODWELL, M.J.W., and BOWERS, J.E.: 'Traveling-wave photodetectors', *IEEE Photonics Technol. Lett.*, 1992, **4**, (12), pp. 1363-1365
- 7 HIETALA, V.M., VAWTER, G.A., BRENNAN, T.M., and HAMMONS, B.E.: 'Traveling-wave photodetectors for high-power, large bandwidth applications', *IEEE Trans.*, 1995, **MTT-43**, (9), pp. 2291-2298
- 8 LIN, K.Y., WU, M.C., ITOH, T., VANG, T.A., MULLER, R.E., SIVCO, D.L., and CHO, A.Y.: 'High-power high-speed photodetectors. Design, analysis, and experimental demonstration', *IEEE Trans.*, 1997, **MTT-45**, pp. 1320-1331
- 9 CHAU, T., FAN, L., TONG, D., MATAHI, S., and WU, M.C.: 'Long wavelength velocity-matched distributed photodetectors'. IEEE conference on *Lasers and electro-optics*, CLEO'98, San Francisco, USA, May 1998
- 10 PASLASKY, J.S., CHEN, P.C., CHEN, J.S., GEE, C.M., and BAR-CHAIM, N.: 'High-power microwave photodiode for improving performance of rf fiber optic links'. Proceedings of conference of the International Society for Optical Engineering, 1996, Vol. 2844, pp. 110-119
- 11 AVERIN, S.V., KOHL, A., MULLER, R., WISSERAND, J., and HEIME, K.: 'Quasi-Shottky barrier MSM-diode on  $n$ -GaS- $UB_{0.47}In_{0.53}As$  using a depleted  $p^+$ - $Ga_{0.47}In_{0.53}As$  layer grown by LP-MOVPE', *Solid State Electron.*, 1993, **36**, (1), pp. 61-67
- 12 LEE, D.H., and LI, S.S.: 'High quality  $In_{0.53}Ga_{0.47}As$  Schottky diode formed by graded superlattice of  $In_{0.53}Ga_{0.47}As/In_{0.52}Al_{0.48}As$ ', *Appl. Phys. Lett.*, 1989, **54**, (19), pp. 1863-1865
- 13 BORN, M., and WOLF, E.: 'Principles of optics' (Pergamon, New York, 1959)
- 14 BONANI, F., and GHIONE, G.: 'On the application of the Kirchhoff transformation to inhomogeneous structures', *Solid-State Electron.*, 1995, **38**, (7), pp. 1409-1412
- 15 NESPOLA, A., CHAU, T., PIROLA, M., WU, M.C., GHIONE, G., and NALDI, C.U.: 'Failure analysis of travelling wave MSM distributed photodetectors'. To be presented at IEEE international *Electron devices meeting*, IEDM'98, San Francisco, CA, December 1998
- 16 JOYCE, W.B.: 'Thermal resistance of heat sinks with temperature dependent conductivity', *Solid-State Electron.*, 1975, **18**, pp. 321-322
- 17 SKRIMSHIRE, C.P., FARR, J.F., SLOAN, D.F., ROBERTSON, R.M., PUTLAND, P.A., STOKOE, I.C.D., and SUTHERLAND, R.R.: 'Reliability of mesa and planar InGaAs PIN photodiodes', *IEE Proc. J. Optoelectron.*, 1990, **137**, (1), pp. 74-78